3D Mixed-Mode Delamination Fracture Criteria–An Experimentalist's Perspective

James R. Reeder

ABSTRACT

Many delamination failure criteria based on fracture toughness have been suggested over the past few decades, but most only covered the region containing mode I and mode II components of loading because that is where toughness data existed. With new analysis tools, more 3D analyses are being conducted that capture a mode III component of loading. This has increased the need for a fracture criterion that incorporates mode III loading. The introduction of a pure mode III fracture toughness test has also produced data on which to base a full 3D fracture criterion. In this paper, a new framework for visualizing 3D fracture criteria is introduced. The common 2D power law fracture criterion was evaluated to produce unexpected predictions with the introduction of mode III and did not perform well in the critical high mode I region. Another 2D criterion that has been shown to model a wide range of materials well was used as the basis for a new 3D criterion. The new criterion is based on assumptions that the relationship between mode I and mode III toughness is similar to the relation between mode I and mode II and that a linear interpolation can be used between mode II and mode III. Until mixed-mode data exists with a mode III component of loading, 3D fracture criteria cannot be properly evaluated, but these assumptions seem reasonable.

INTRODUCTION

Delamination is a primary failure mode of laminated composite materials. Delaminations and their susceptibility to growth are normally characterized using fracture mechanics principles and the strain energy release rate parameter (G) [1, 2]. The critical value of strain energy release rate, the fracture toughness (G_c), is dependent on both the material and the manner in which the delamination is loaded. Three orthogonal modes of loading are considered and include mode I (opening), mode II (sliding shear), and mode III (tearing shear) as shown in Figure 1. A delamination may be loaded in one of these modes, or more likely, it will be loaded in some combination of these modes. The critical strain energy release rate (G_c) at which the delamination actually begins to extend has been shown to vary significantly depending on the mode of loading [3].

NASA Langley Research Center, M/S 188E, Hampton VA 23681-2199, USA

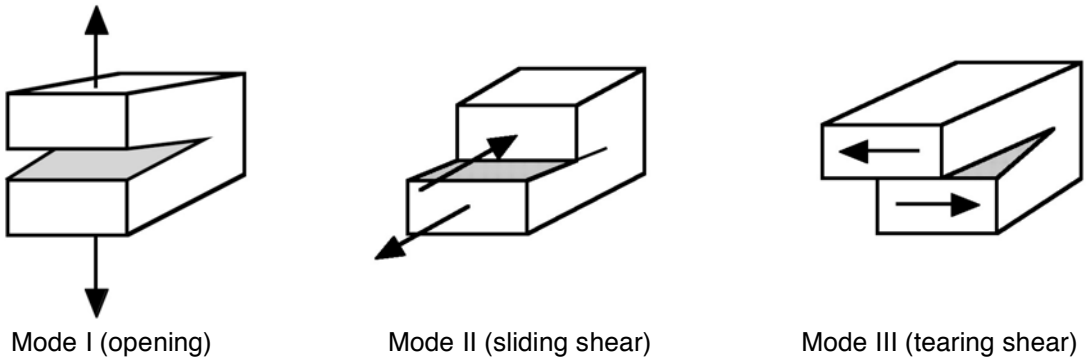

Figure 1. Pure Mode Loadings.

To determine the fracture toughness (G_c) for various loading states, testing is performed to measure the G_c under known loading conditions. ASTM has created standards or is working on standards to measure G_c under a variety of loading conditions. The ASTM standard for mode I loading (ASTM D5528) uses the double cantilever beam (DCB) test to measure the pure mode I fracture toughness (G_{Ic}) [4]. ASTM is also working to standardize the End Notch Flexure (ENF) test [5, 6] for pure mode II fracture toughness (G_{IIc}). The mixed-mode bending (MMB) test is an ASTM standard (ASTM D6671) that can measure fracture toughness over a wide range of combinations of Mode I and Mode II loading [7, 8]. For pure mode III, the Edge Crack Torsion Test (ECT) (also a test that ASTM is working to standardize) can be used to measure fracture toughness [9, 10]. No mixed-mode test is known to have been developed that measures fracture toughness with a uniform mode III component across the delamination front. An essentially uniform mixed-mode component is needed so that a single fracture toughness calculated from measured test parameters can be assumed to apply uniformly to the entire delamination front.

It is not practical to test all mixed-mode combinations, so it is important to define a fracture criterion that correctly establishes the critical fracture toughness (G_c) at mode combinations that have not been tested. This is particularly true in finite element modeling of delaminations where the resulting loading mode at each node may be any combination of the three orthogonal loading modes. Although many of the fracture criteria that have been suggested are based on some physical phenomenon, an understanding of the actual mechanisms that control the value of G_c as a function of loading mode is not well established. Therefore, each of the fracture criteria that will be discussed should be viewed as a curve fit to fracture toughness test data.

Since all of the fracture criteria can be viewed as curve fits to data, one could argue that the form of the fracture criterion does not matter as long as the critical surface described by the mathematical criterion equations fit the data. But criteria do vary and often have different numbers of parameters that are used to fit the data. Too few parameters can result in a criterion that is not capable of adequately

describing the material response. Too many parameters can allow curve fits that produce radical undulations as the curve is fit to data that has experimental error and produce unrealistic responses in regions where there is no (or little) experimental data. If the criterion has the wrong mathematical form, it again may not fit the material response well or may produce large variations in response to seemingly minor variations in input parameters. By agreeing on a common fracture criteria, toughness data can easily be translated from the experimentalist performing the toughness testing to analysts who can introduce the material response into their models with just a few material parameters. Additionally, some criteria may be more easily implemented into failure analysis routines than others.

In finite element modeling of delamination growth, the virtual crack closure technique (VCCT) [11, 12] is normally used to calculate the strain energy release rate. In this technique, the forces at the delamination front are combined with the displacements just to the open side of the delamination front to calculate the strain energy release rate. The VCCT has the advantage that not only is the total strain energy release rate calculated, but the mode I, II and III components of strain energy release rate are also calculated (G_I, G_{II}, G_{III}, respectively). Until recently VCCT was normally performed in post processing and often by hand, which made evaluating the criticality of a delamination somewhat tedious. Propagating a delamination was labor intensive because of the manual step of calculating strain energy release rate after each step. Recently the ABAQUS/Standard† commercial finite element code released their implementation of VCCT [13] which is based on a new interface element developed by Boeing [14] that performs the VCCT calculation internally and therefore allows the automation of delamination propagation analyses. Because the VCCT calculation is performed by the code, it also simplifies the analysis of 3D problems where the delamination front is described by a large number of nodes. In 3D problems, delaminations normally have a mode III component while for 2D problems GIII=0. Alternative models for delamination growth such as the decohesion element also rely on fracture toughness and require a 3D fracture criterion [15].

Because most of the fracture toughness data has been limited to the mode I-mode II regime, most fracture criteria were limited to this 2D regime. With the ECT test development for mode III toughness and the new automated FEM routines that make 3D models easier to analyze, the choice of a 3D fracture criterion is becoming more important. In this paper, popular 2D fracture criteria will be reviewed, a method for visualizing 3D fracture criteria will be suggested, 3D fracture criteria will be reviewed, and a new 3D fracture criterion will be introduced and compared to existing criteria.

FRACTURE TOUGHNESS DATA

Mixed mode I–mode II fracture toughness data from four different materials are shown in Figure 2. AS4/3501-6 is a common brittle epoxy composite. IM7/E7T1 is a high strain-to-failure fiber composite with a two phase toughened epoxy matrix. IM7/977-2 has the same high strain-to-failure fiber but with a toughened epoxy matrix, while the AS4/PEEK is the same common fiber as the first composite

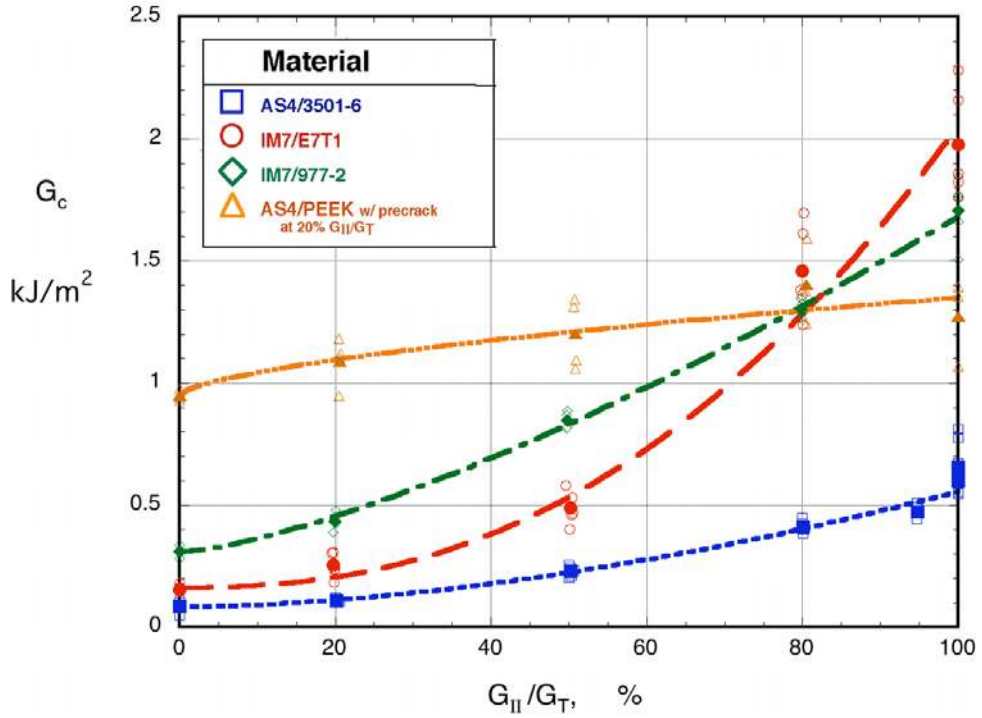

Figure 2. Mixed-mode toughness data for various materials.

but with a thermoplastic resin. The AS4/PEEK data was taken after the specimens were precracked under 20% mode II loading. In the figure, the open symbols are toughness values measured from individual specimens, solid symbols are averages at a given load state, and the curves are curve fits to the data. The criterion used for the curve fits in Figure 2 is based on the B-K 2D fracture criterion [16] that will be discussed later in the paper. These four materials give a significant sampling of the large selection of graphite reinforced polymer composites that are commercially available. From Figure 2, it is clear that the various materials have dramatically different responses when loaded in different mode combinations. The brittle epoxy composite (AS4/3501-6) has significantly lower toughness at all ratios than the other composites tested. AS4/Peek has a much higher mode I toughness but this does not translate to a mode II toughness that is higher than the other materials. AS4/Peek is also noticeably different in shape from the other materials in the mixed-mode region indicating that a different fracture mechanism is probably occurring at the micro-scale. In all of the data presented here, the mode II toughness is significantly larger than the mode I toughness (between 1.5 and 13 times larger). The data was presented in earlier papers [3, 17], but the raw data was reanalyzed to be consistent with the ASTM standards that have since been published.

The mode III toughness has also been measured for a variety of materials. AS4/3501-6 has been reported to be between 0.65 and 0.85 kJ/m^2 [18]. This makes the ratios of pure mode toughness G_{IIc}/G_{Ic}~7 and G_{IIIc}/G_{Ic}~9. Initial indications are that mode III toughness will tend to be higher than mode II which is higher than mode I. One glass/toughened epoxy composite was reported to have pure mode

toughness ratios of 3.3 and 4.3 for G_{IIc}/G_{Ic} and G_{IIIc}/G_{Ic}, respectively [19]. A toughened epoxy with a high modulus fiber is reported to have pure mode toughness ratios of 7 and 7 for G_{IIc}/G_{Ic} and G_{IIIc}/G_{Ic}, respectively, while the same resin with glass fibers had ratios of 7 and 13 for G_{IIc}/G_{Ic} and G_{IIIc}/G_{Ic}, respectively [10, 20].

The high mode I region is generally presumed to be the most critical region of a delamination fracture criterion for most structures. Many of the structures with delaminations that have been analyzed have had a sizeable mode I component over at least part of the delamination front when the structure was loaded. The sizeable mode I component coupled with the fact the toughness in the high mode I region is normally significantly less than in the other mixed-mode regions means that it is normally a delamination loaded with a high mode I component that becomes critical first.

TWO DIMENSIONAL MIXED-MODE CRITERIA

Many delamination fracture criteria were developed before there were consistent sets of mixed-mode experimental data with which to compare. Once delamination toughness tests were developed for mode I and mode II and eventually mixed-mode I and II, it was clear that the fracture toughness was not constant but changed significantly depending on the mixed-mode ratio. With the mixed-mode data for different materials being available, fracture criteria could finally be evaluated for how well they matched the experimental data. Early representations of the mixed mode response were generally made by dividing the critical toughness value into its mode I and mode II components (G_I and G_{II}, respectively) and plotting this locus of points on a Cartesian coordinate system to define the fracture curve as shown in Figure 3. The same data from Figure 2 is re-plotted in what will be referred to as the "early" format.

The representation of the fracture criteria in this form influenced the development of fracture criteria by pushing them toward terms which compared the mode component directly to a pure mode toughness. For example, the power law criterion [21] given by equation 1 contains the G_I/G_{Ic} and G_{II}/G_{IIc} terms. Mathematically this criterion and the other criteria presented in this paper will be presented in a form where the delamination is expected to grow when a fracture parameter becomes greater than unity.

$$\left(\frac{G_I}{G_{Ic}}\right)^{\alpha} + \left(\frac{G_{II}}{G_{IIc}}\right)^{\beta} \geq 1 \qquad (1)$$

This representation of the data shows a fracture curve in all of the epoxy composites (AS4/3501-6, IM7/E7T1, and IM7/977-2) where the mode I component actually increases with the introduction of a small amount of mode II. This complex response in the high mode I region turned out to be a phenomenon that was not captured well by many of the suggested mixed-mode criteria and is probably an artifact of the artificial division of the fracture toughness into individual component modes.

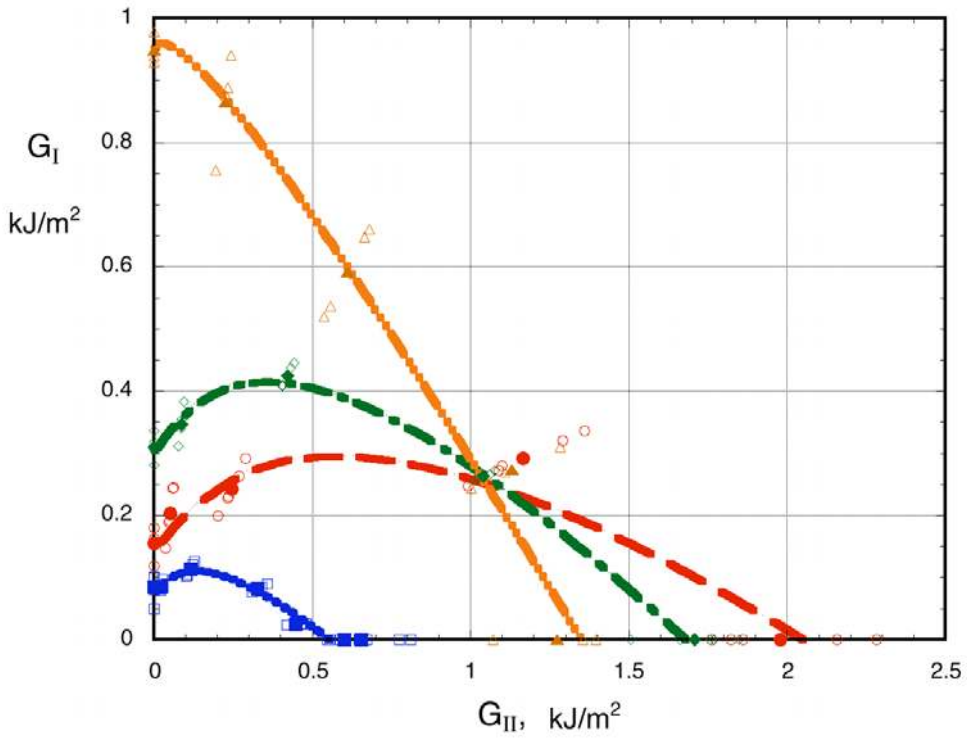

Figure 3. Early representation of 2D fracture criteria.

O'Brien [22] suggested that that it would be more appropriate for the data to presented as the critical fracture toughness G_c vs. the proportion of mode I or mode II loading as seen in Figure 2. This seemed more appropriate because the critical toughness components were not independent of each other and in testing it is normally the mode mixety that is controlled and the critical fracture toughness that is measured. As seen in Figure 2, an additional advantage is that the fracture data appears to have a much more regular shape. The mathematical expressions for the curves in Figure 2 and Figure 3 are identical.

Table 1 shows quite a number of the 2D mixed-mode criteria that have been suggested over time. The terms G_{Ic}, G_{IIc}, G_c, α, β, η, ξ, ζ, κ, φ, γ, ρ, τ, χ, ρ, and τ are all material parameters that are used by the different criteria to fit the experimental data. G_T is the sum of the strain energy release rate components (in the 2D case $G_T=G_I+G_{II}$).

All of these criteria except for the B-K criterion were reviewed in an earlier paper [3], based on how many curve fitting parameters were used, how well the criterion fit a variety of material responses and whether the criterion was of a form that could be easily used. In that paper, the bilinear criterion and linear interaction criterion, which is a simplification of the power law criterion, were recommended.

The B-K criterion [33], which was introduced after the earlier review paper, is used in Figure 2 and Figure 3 to produce the plotted curve fits to data and can be seen to fit the wide range of material responses. The B-K criterion only uses 3 curve fitting parameters (G_{Ic}, G_{IIc} and η). The parameters used for the B-K curve fits are shown in Table 2 along with the parameters used for the power law criterion. The B-K criterion has been adopted by a number of researchers studying delamination growth [15, 34-36].

TABLE 1. TWO-DIMENSIONAL MIXED-MODE FRACTURE CRITERIA

Criterion Name	**Criterion Equation**
mode I critical [21]	$G_I / G_{Ic} \geq 1$
mode II critical [23]	$G_{II} / G_{IIc} \geq 1$
G_T critical [24]	$G_T / G_c \geq 1$
Power Law[21]	$\left(\frac{G_I}{G_{Ic}}\right)^{\alpha} + \left(\frac{G_{II}}{G_{IIc}}\right)^{\beta} \geq 1$
Polynomial interaction[25]	$\frac{G_T}{G_{Ic} + \rho\left(\frac{G_{II}}{G_I}\right) + \tau\left(\frac{G_{II}}{G_I}\right)^2} \geq 1$
K_I critical[26]	$\frac{G_T}{G_{IIc} - (G_{IIc} - G_{Ic})\sqrt{\frac{G_I}{G_{Ic}}}} \geq 1$
Hackle[27]	$\frac{G_T}{(G_{Ic} - \chi) + \chi\sqrt{1 + \frac{G_{II}}{G_I}\sqrt{\frac{E_{11}}{E_{22}}}}} \geq 1$
Exponential Hackle[28]	$\frac{G_T}{(G_{Ic} - G_{IIc}) + e^{\gamma(1-N)}} \geq 1 \quad where\ N = \sqrt{1 + \frac{G_{II}}{G_I}\sqrt{\frac{E_{11}}{E_{22}}}}$
Exponential K ratio[29]	$\frac{G_T}{G_{Ic} + (G_{IIc} - G_{Ic})e^{\eta\sqrt{G_{II}/G_I}}} \geq 1$
Crack Opening Displacement critical[30] Mode I: Mode II:	$\frac{G_{II}}{\frac{1}{3}G_{IIc}\sqrt{\frac{E_{11}}{E_{22}}}\left(\frac{G_{Ic}}{G_I} - \frac{G_I}{G_{Ic}}\right)} \geq 1$ $\frac{G_I}{3G_{Ic}\sqrt{\frac{E_{22}}{E_{11}}}\left(\left(\frac{G_{IIc}}{G_{Ic}}\right)^2\left(\frac{G_{Ic}}{G_{II}}\right) - \left(\frac{G_{II}}{G_{Ic}}\right)\right)} \geq 1$
Mixed-Mode Interaction[31]	$\frac{G_I}{G_{Ic}} + (\kappa - 1)\frac{G_I}{G_{Ic}}\frac{G_{II}}{G_{IIc}} + \frac{G_{II}}{G_{IIc}} \geq 1$
Linear %G interaction[32]	$\frac{G_I}{G_{Ic}} + \left(\kappa - 1 + \varphi\left(\frac{1}{1 + \frac{G_{II}}{G_I}}\right)\right)\frac{G_I}{G_{Ic}}\frac{G_{II}}{G_{IIc}} + \frac{G_{II}}{G_{IIc}} \geq 1$
Bilinear interaction[3]	$\frac{G_I - \xi G_{II}}{G_{Ic}} \geq 1 \quad for\ \frac{G_{II}}{G_I} < \frac{\frac{1}{\xi}G_{Ic} + G_{IIc}}{G_{Ic} + \xi G_{IIc}}$ $\frac{\zeta G_{II} - G_I}{\zeta G_{IIc}} \geq 1 \quad for\ \frac{G_{II}}{G_I} > \frac{\frac{1}{\xi}G_{Ic} + G_{IIc}}{G_{Ic} + \xi G_{IIc}}$
B-K Criterion[16, 33]	$\frac{G_T}{G_{Ic} + (G_{IIc} - G_{Ic})\left(\frac{G_{II}}{G_T}\right)^{\eta}} \geq 1$

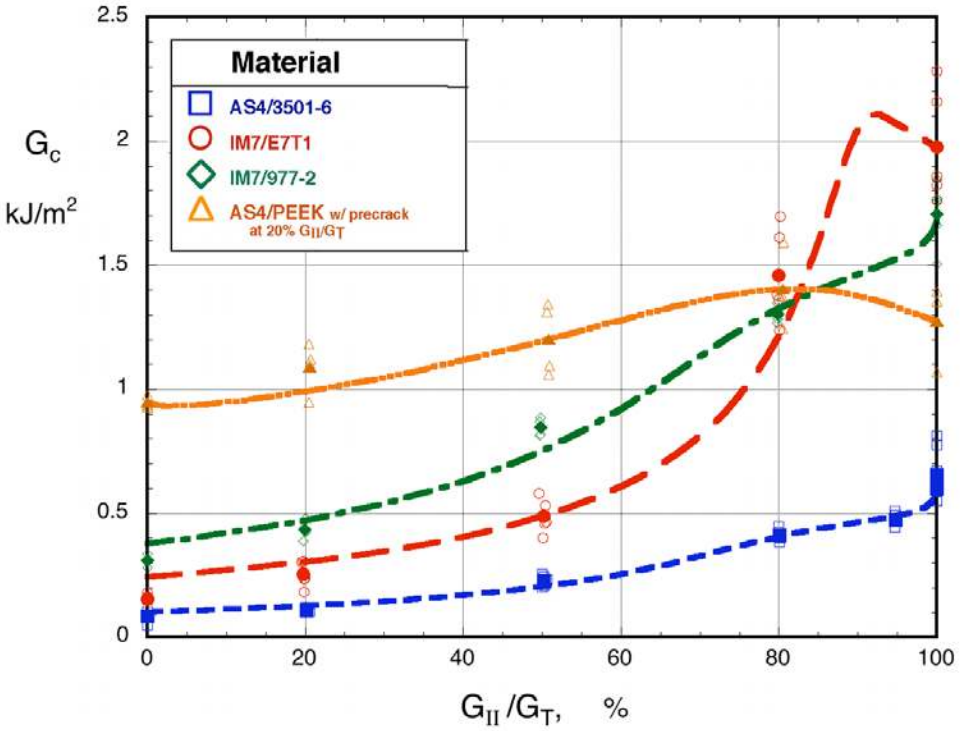

Figure 4. Power Law fit to experimental data.

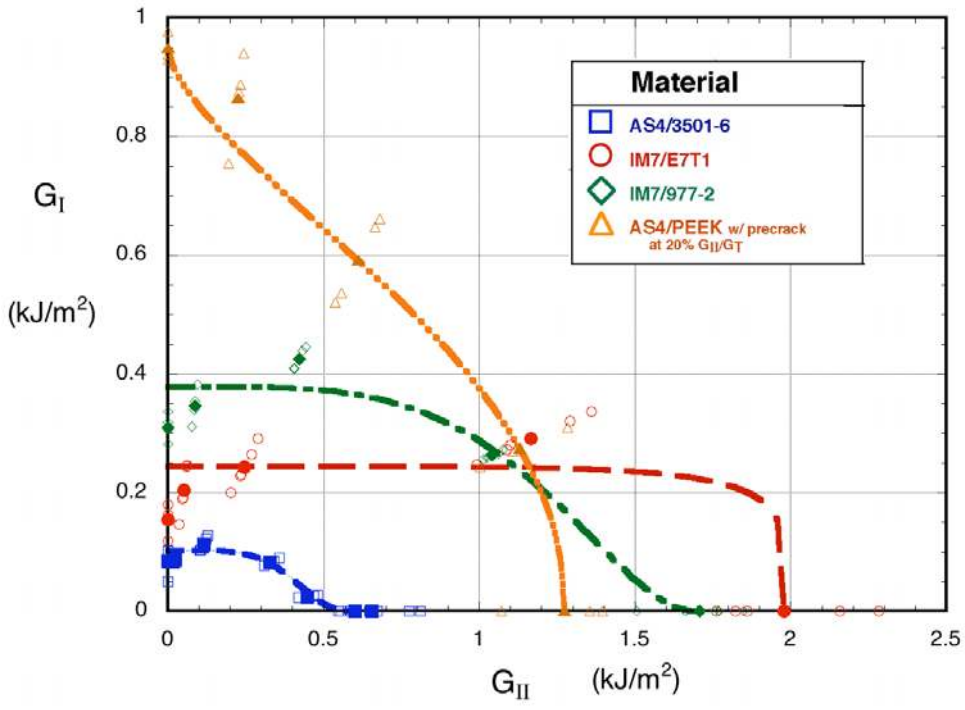

Figure 5. Power Law fit to experimental data, "early" format.

TABLE 2. 2D CRITERIA PARAMETERS

Material	B-K Criterion			Power Law Criterion			
	G_{Ic} (kJ/m^2)	G_{IIc} (kJ/m^2)	η -	G_{Ic} (kJ/m^2)	G_{IIc} (kJ/m^2)	α -	β -
AS4/3501-6	0.0816	0.554	1.75	0.103	0.648	0.17	4.8
IM7/E7T1	0.161	2.05	2.35	0.244	1.98	6	6
IM7/977-2	0.306	1.68	1.39	0.379	1.70	0.49	3.9
AS4/PEEK	0.949	1.35	0.63	0.948	1.273	2.1	0.62

For comparison, the Power Law criterion, which is one of the early and more popular criteria, is shown in Figure 4 and Figure 5, plotted in the current and "early" format, respectively. In Figure 5, it is clear that this criterion is not able to capture the rising mode I component in the low mode II region. This is not as obvious when the data is plotted in Figure 4, but the IM7/E7T1 curve does have a peak in the high mode II region that seems unexpected for an actual material response. The power law criterion is also difficult to express in terms of the mixed-mode ratio (G_{II}/G_T).

3D DIMENSIONAL REPRESENTATION OF FRACTURE TOUGHNESS

With the addition of Mode III contributions to toughness, understanding the material response becomes more complicated. To facilitate understanding the toughness response to Mode III, a variety of different visualizations of 3D fracture critical surfaces can be made as shown in Figure 6. Throughout Figure 6, the mode I-mode II fracture curve is highlighted with a heavy black line. Figure 6a shows an extension of the original method of presenting mixed-mode data where a critical value of toughness is divided into three mode components and then the components are plotted on a Cartesian coordinate system. This division of the critical modes probably makes less sense in 3D than it did for the 2D fracture visualization because it is now artificially dividing the toughness three ways instead of two. A second way of visualizing the data would be to plot the percentage of mode II and percentage of mode III on the X and Y axis, respectively, and then the Z axis becomes the critical fracture toughness as seen in Figure 6b. The base of this coordinate system was really a right triangle since half of the base plane is not used. For example, it is not possible to have delamination load state that is both 100% mode II and 100% mode III. This visualization is a reasonable representation of the fracture criterion, but it does not communicate well that mode I, mode II, and mode III are all comparable orthogonal modes of loading. To communicate this in a better way, one can go to a non-Cartesian coordinate system such as the one shown in Figure 6c. The base of this coordinate system is an equilateral triangle with each of the 3 corners describing a pure mode state. Figure 6c provides a good representation of the fracture critical surface, but it is difficult to read a toughness at

a specific load state off of this type of 3D chart. In order to read toughness values at specific load states, a collection of curves can be taken off of the 3D surface and plotted on a 2D chart. Although one might choose various curves to represent the 3D surface, choosing the collection of curves at constant total shear percentage makes a good choice because of the assumed importance of mode I loading. This set of curves is shown in Figure 6d. In this form, one can calculate the % total shear, $(G_{II} + G_{III})/G_T$, to find the correct location on the x-axis. Then, by interpolating between the closest two ratios of $G_{II}/(G_{II}+G_{III})$ one can read a value of toughness from the chart. Once data is available, data sets measured at different ratios of $G_{II}/(G_{II}+G_{III})$ can also be plotted and compared to curves from a 3D fracture criterion. When attempting to understand what is being described by a

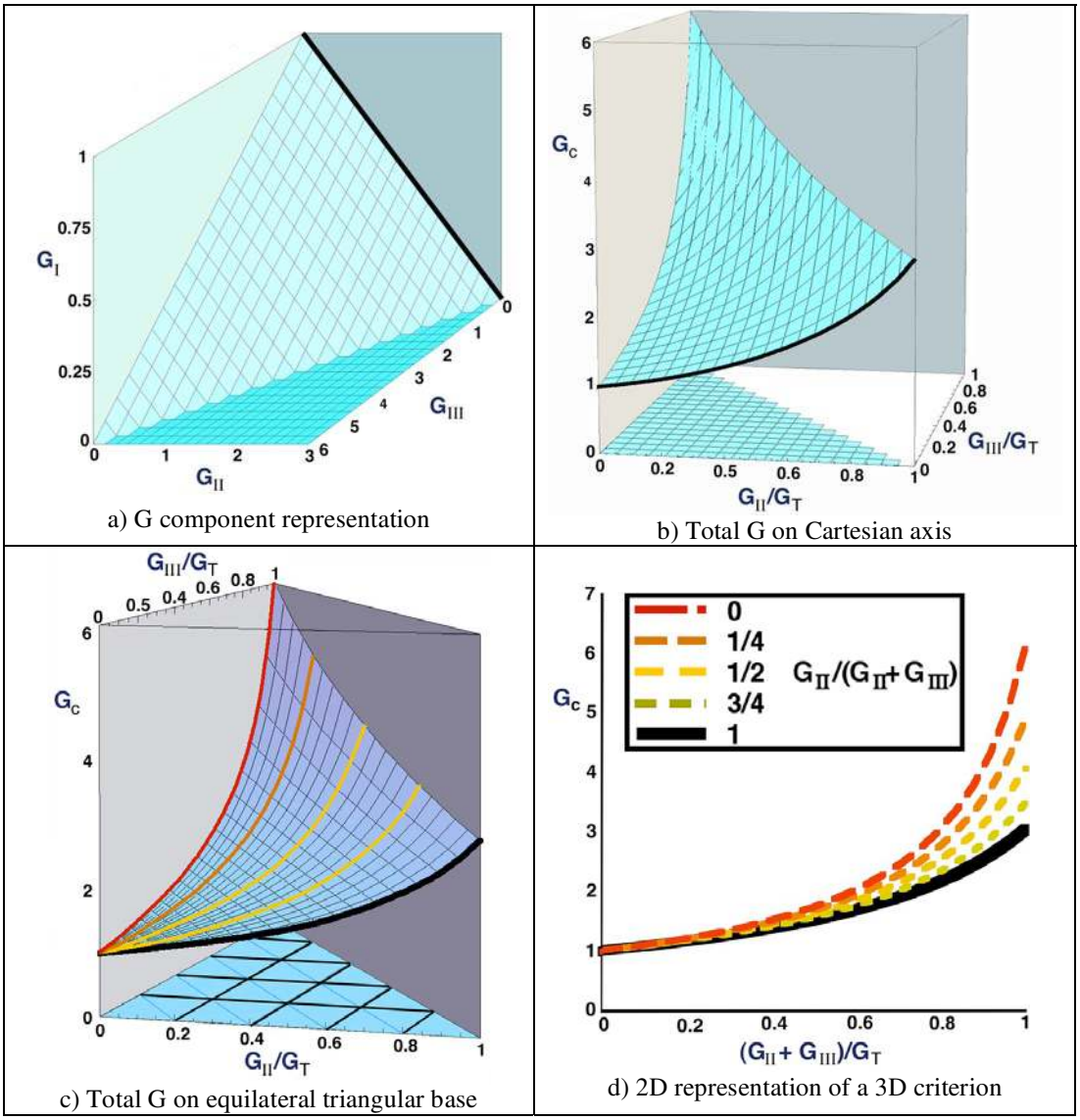

a) G component representation

b) Total G on Cartesian axis

c) Total G on equilateral triangular base

d) 2D representation of a 3D criterion

Figure 6. Representation of 3D fracture critical surfaces.

fracture criterion equation, both the 3D representation in Figure 6c and the 2D representation of Figure 6d can prove useful, so both representations will be used through the rest of the paper.

3D DELAMINATION FRACTURE CRITERIA

Modified Use of 2D Criteria

Even before mode III data was available, FEM analyses of delaminations were predicting delamination load states that contained a mode III component which created a problem when trying to make delamination growth predictions. Often mode III was grouped with mode II and then this combined shear component of G was substituted into one of the 2D fracture criteria presented earlier. An example of this substitution is shown in Equation 2 where the power law was used as the initial 2D fracture criteria:

$$\left(\frac{G_I}{G_{Ic}}\right)^{\alpha} + \left(\frac{G_{II} + G_{III}}{G_{IIc}}\right)^{\beta} \geq 1 \tag{2}$$

With the introduction of the Edge Crack Torsion Test (ECT) and thus pure mode III data that was significantly different from pure mode II data, it became apparent that these criteria were no longer satisfactory.

3D Power Law Criterion

The 2D power law delamination criterion is one of the more popular 2D criteria and was easily extended to 3D as shown in Equation 3 [37].

$$\left(\frac{G_I}{G_{Ic}}\right)^{\alpha} + \left(\frac{G_{II}}{G_{IIc}}\right)^{\beta} + \left(\frac{G_{III}}{G_{IIIc}}\right)^{\chi} \geq 1 \tag{3}$$

This fracture criterion uses six fitting parameters to describe the fracture critical surface (G_{Ic}, G_{IIc}, G_{IIIc}, α, β, χ) so a large number of different responses can be represented. Figure 7 shows a selection of fracture critical surfaces from this criterion. Throughout the figure, G_{Ic}, G_{IIc}, and G_{IIIc} are set to 1, 3, and 6, respectively. This is generic to any material with pure mode ratios of 3 and 6 (G_{IIc}/G_{Ic} and G_{IIIc}/G_{Ic}, respectively) which are reasonable values given the range of material responses discussed previously. Figure 7a is actually the linear interaction criterion where all the exponents are set to 1. Notice that although this is called a linear interaction no part of the contour appears linear in this view. As seen in Figures 7d and 7e, the criterion often predicts mixed-mode toughness values that are higher or lower than any of the pure mode states. These values seem suspect indicating a deficiency in the criterion. Even with 6 curve fitting parameters, the criterion was also not able to model a convex shape near the high mode I region that is indicative of the material response seen in IM7/PEEK material data set presented in Figure 3. Although the other material data sets were concave in this region, from the 2D analyses, it is clear that even with these materials the power law had trouble

a	$G_{Ic}=1$ $G_{IIc}=3$ $G_{IIIc}=6$ $\alpha=1$ $\beta=1$ $\chi=1$	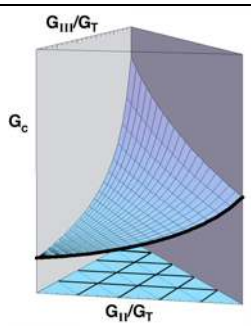	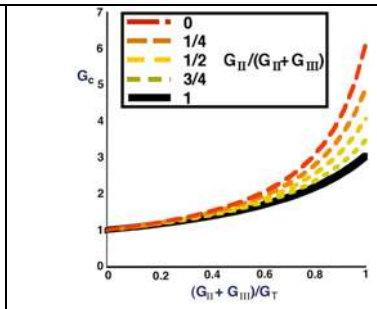
b	$G_{Ic}=1$ $G_{IIc}=3$ $G_{IIIc}=6$ $\alpha=2$ $\beta=1$ $\chi=1$	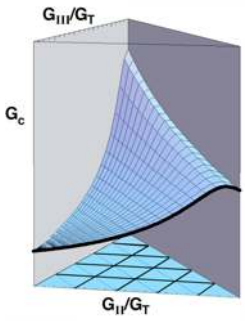	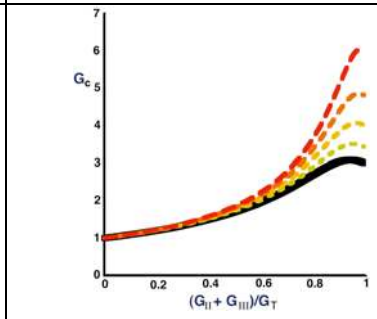
c	$G_{Ic}=1$ $G_{IIc}=3$ $G_{IIIc}=6$ $\alpha=0.5$ $\beta=1$ $\chi=1$	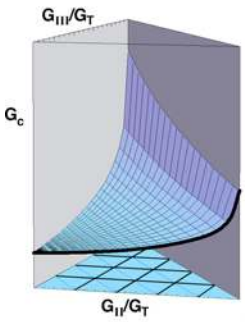	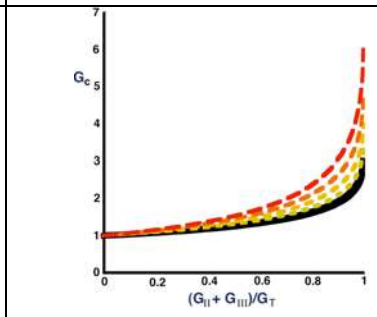
d	$G_{Ic}=1$ $G_{IIc}=3$ $G_{IIIc}=6$ $\alpha=2$ $\beta=2$ $\chi=2$	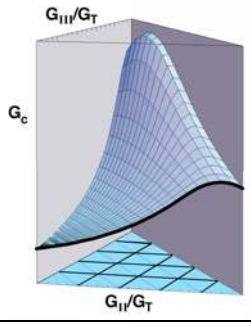	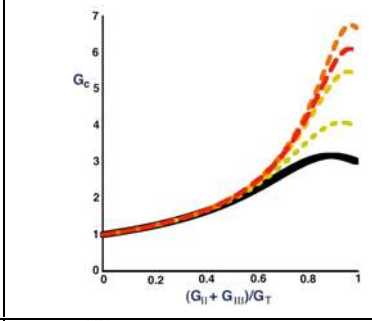
e	$G_{Ic}=1$ $G_{IIc}=3$ $G_{IIIc}=6$ $\alpha=0.5$ $\beta=0.5$ $\chi=0.5$	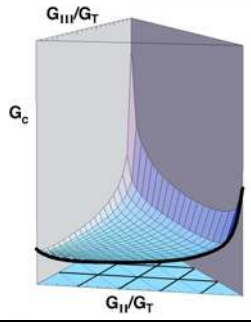	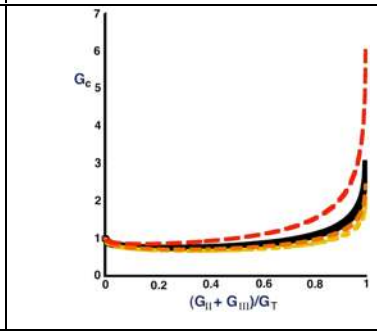

Figure 7. 3D Power law representation.

matching the data in the critical high mode I region. This deficiency would not have improved with the introduction of mode III.

By using the 3D Power Law criterion and setting $\chi=\beta$ which was curve fit to mode I–mode II data, an unexpected fracture critical contour would be created (e.g., the 3D criterion in Figure 7d is far from an extrapolation of the G_I-G_{II} curve). The unexpected fracture critical contour would of course produce unexpected delamination predictions. Futher, it should be noted that equation 3 does not reduce to equation 2 by making $G_{IIc}=G_{IIIc}$ and $\chi=\beta$.

New 3D Failure Criterion.

Because the B-K criterion fits the 2D data well, it is an obvious choice as the basis for a 3D criterion. A straightforward extension of the 2D criterion results in the 3D fracture criteria given by equation 4. However, when the equation is evaluated by plotting as suggested earlier, values of exponents in the range used to fit the 2D data in Table 1 quickly lead to values of mixed-mode toughness that were lower than any of the pure mode toughnesses, as seen in Figure 8. Again, this response has no precedent in the 2D data and seems suspect.

$$\frac{G_T}{G_{Ic}+\left(G_{IIc}-G_{Ic}\right)\left(\frac{G_{II}}{G_T}\right)^{\eta}+\left(G_{IIIc}-G_{Ic}\right)\left(\frac{G_{III}}{G_T}\right)^{\varsigma}}\geq 1 \qquad (4)$$

ECT data only provides pure mode III toughness data that has shown that mode III toughness is normally higher than mode II toughness. There is no accepted test and therefore no data that shows how the toughness changes as the mode III component is increased, e.g. nothing that defines the shape of the curve between mode I and mode III. If we assume that the response to mode III will be similar to mode II since they are both shear types of loading, then the fracture criterion in the

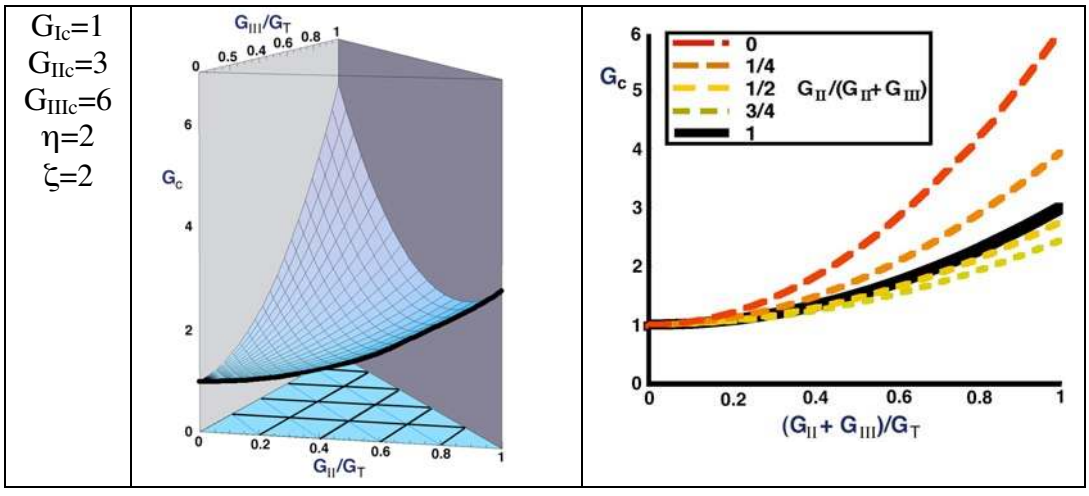

Figure 8. 3D representation of rejected criterion (equation 5).

mode I–mode III plane might be given by equation 6 which is a modification of the B-K criterion but with G_{II} terms replaced by G_{III} terms.

$$\frac{G_T}{G_{Ic} + \left(G_{IIIc} - G_{Ic}\right)\left(\frac{G_{III}}{G_T}\right)^{\eta}} \geq 1 \tag{5}$$

Since there is no data available to base the description of how the mode II and mode III loadings interact, a reasonable supposition is that a linear interpolation governs this interaction. By combining these assumptions and performing the appropriate algebra, the suggested fracture criterion becomes:

$$\frac{G_T}{G_{Ic} + \left(G_{IIc} - G_{Ic}\right)\left(\frac{G_{II} + G_{III}}{G_T}\right)^{\eta} + \left(G_{IIIc} - G_{IIc}\right)\frac{G_{III}}{G_{II} + G_{III}}\left(\frac{G_{II} + G_{III}}{G_T}\right)^{\eta}} \geq 1 \tag{6}$$

The criterion can be rewritten as shown in equation 7 to show the symmetry between mode II and mode III.

$$\frac{G_T}{G_{Ic} + \left(\left(G_{IIc} - G_{Ic}\right)\frac{G_{II}}{G_T} + \left(G_{IIIc} - G_{Ic}\right)\frac{G_{III}}{G_T}\right)\left(\frac{G_{II} + G_{III}}{G_T}\right)^{\eta-1}} \geq 1 \tag{7}$$

This new 3D criterion is shown in Figure 9 for a variety of inputs. Notice that relationship between mode II and mode III at a given % total shear is always linear. The problems encountered with the Power Law criterion where the mixed-mode toughness was higher than any of the pure mode toughnesses was also avoided. This fracture criterion has already been implemented as part of the VCCT for ABAQUS routines[38] and is being used to analyze delaminations in complicated 3D structures [39]. This simple extrapolation into the 3D plane is believed to be all that can be justified until tests are developed to measure mixed-mode fracture toughness with known percentages of mode III.

CONCLUDING REMARKS

Common delamination fracture criteria available in the literature have been reviewed. Most of these are 2D criteria used for making predictions in the mode I–mode II region of loading because fracture toughness data exists primarily in this region. With more automated methods of analyzing delaminations, full 3D analysis of delaminations (which contain a mode III component) are becoming more common and require a 3D fracture criterion. Evaluation of fracture criteria in the past has been influenced by how the toughness data is presented. A framework for presenting 3D fracture criteria was suggested and an evaluation of the traditional power law fracture criterion showed deficiencies in the responses that could be predicted with this criterion. A new 3D fracture criterion was introduced based on a

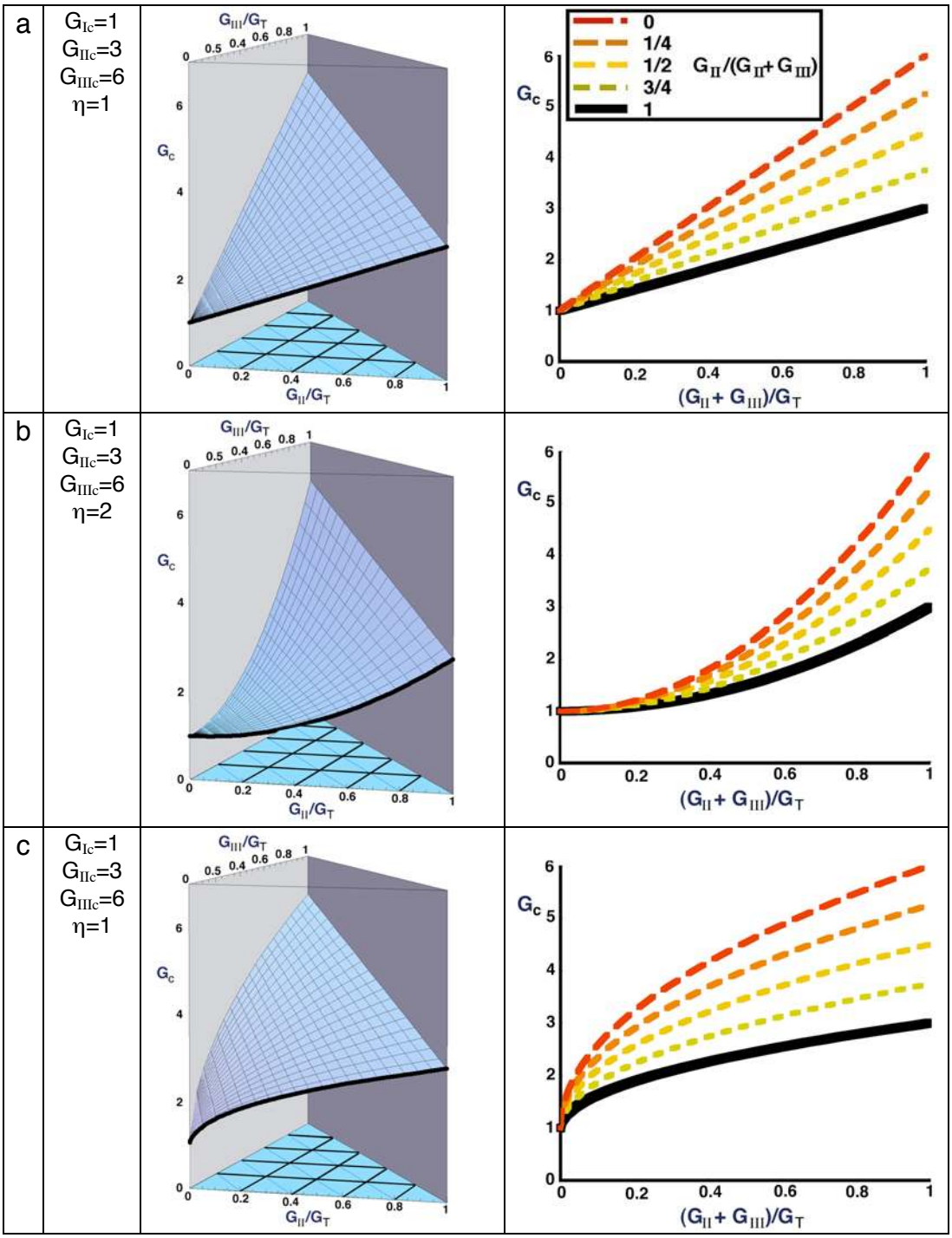

Figure 9. 3D representation of proposed criterion.

2D fracture criterion that has been shown to model a wide range of materials well in the mode I–mode II region. The new criterion is based on the supposition that the relationship between mode I and mode III toughness is similar to the relation between mode I and mode II toughness and that a linear interpolation can be used between mode II and mode III. A proper evaluation of the new criterion will have to wait until mixed-mode fracture tests are developed that incorporate a mode III component of loading.

REFERENCES

1. O'Brien, T.K. 2001. "Fracture Mechanics of Composite Delamination," in *ASM Handbook, Volume 21, Composites*. ASM International. pp. 241-245.
2. Tay, T.E. 2003. "Characterization and Analysis of Delamination Fracture in Composites - an Overview of Developments from 1990 to 2001." *Appl Mech Rev*, 56(1):1-32.
3. Reeder, J.R. 1993. "A Bilinear Failure Criterion for Mixed-Mode Delamination," in *Composite Materials: Testing and Design (Eleventh Volume), ASTM STP 1206*, E.T. Camponeschi, Jr., Ed. ASTM Int., W. Conshohocken, PA. pp. 303-322.
4. ASTM Standard D5528, "Test Method for Mode I Interlaminar Fracture Toughness of Unidirectional Fiber-Reinforced Polymer Matrix Composites." *Annual Book of ASTM Standards, Vol. 15.03*. ASTM Int., W. Conshohocken, PA.
5. Russell, A.J. 1982. "On the Measurement of Mode II Interlaminar Fracture Energies." Material Report 82-O. DREP.
6. Davidson, B.D. and X. Sun. 2005. "Effects of Friction, Geometry, and Fixture Compliance on the Perceived Toughness from Three- and Four-Point Bend End-Notched Flexure Tests." *J Reinf Plas & Comp*, 24(15):1611-1628.
7. ASTM Standard D6671, "Test Method for Mixed Mode I-Mode II Interlaminar Fracture Toughness of Unidirectional Fiber Reinforced Polymer Matrix Composites." *Annual Book of ASTM Standards, Vol. 15.03*. ASTM Int., W. Conshohocken, PA.
8. Reeder, J.R. and J.H. Crews. 1992. "Redesign of the Mixed-Mode Bending Delamination Test to Reduce Nonlinear Effects." *J Comp Tech Res*, 14(1):12-19.
9. Lee, S.M. 1993. "An Edge Crack Torsion Method for Mode III Delamination Fracture Testing." *J Comp Tech Res*, 15(3):193-201.
10. Ratcliffe, J. 2004. "Characterization of the Edge Crack Torsion (ECT) Test for Mode III Fracture Toughness Measurement of Laminated Composites," in proceeding of the *19th ASC/ASTM Technical Conference*. Atlanta.
11. Rybicki, E.F. and M.F. Kanninen. 1977. "A Finite Element Calculation of Stress Intensity Factors by a Modified Crack Closure Integral." *Eng Frac Mech*, 9:931-938.
12. Krueger, R. 2004. "Virtual Crack Closure Technique: History, Approach and Applications." *Appl Mech Rev*, 57(2):109-143.
13. ABAQUS Analysis User's Manual - Version 6.5. 2005. Vol. I: ABAQUS Inc.
14. Mabson, G., B. Doper, and L. Deobald. 2004. "User Manual for Fracture and Traction Interface Elements-Version 1.3." The Boeing Company.
15. Camanho, P.P., C.G. Davila, and S.T. Pinho. 2004. "Fracture Analysis of Composite Co-Cured Structural Joints Using Decohesion Elements." *Fat & Frac Eng Mat & Struc*, 27(9):745-757.
16. Benzeggagh, M.L. and M. Kenane. 1996. "Measurement of Mixed-Mode Delamination Fracture Toughness of Unidirectional Glass/Epoxy Composites with Mixed-Mode Bending Apparatus." *Comp Sci & Tech*, 56(4):439-449.
17. Reeder, J.R. 2003. "Refinements to the Mixed-Mode Bending Test for Delamination Toughness." *J Comp Tech Res*, 25(4):191-195.
18. Liao, W.C. and C.T. Sun. 1996. "The Determination of Mode III Fracture Toughness in Thick Composite Laminates." *Comp Sci & Tech*, 56(4):489-499.
19. Li, J., et al. 1997. "Evaluation of the Edge Crack Torsion (ECT) Test for Mode III Interlaminar Fracture Toughness of Laminated Composites." *J Comp Tech Res*, 19(3):174-183.

20. Hansen, P. and R. Martin. 1999. "DCB, 4ENF and MMB Delamination of S2/8552 and Im7/8552." N68171-98-M-5177. Materials Engineering Research Laboratory Ltd. (MERL).
21. Whitcomb, J.D. 1984. "Analysis of Instability-Related Growth of a through-Width Delamination." NASA TM-86301.
22. O'Brien, T.K., et al. 1983. "Determination of Interlaminar Fracture Toughness and Fracture Mode Dependence of Composites Using the Edge Delamination Test," in proceeding of the *International Conference on Testing, Evaluation and Quality Control of Composites*. Quildford, England, pp. 223-242.
23. Gillespie, J.W., Jr., et al. 1985. "Delamination Growth in Composite Materials." NASA CR-176416.
24. Wu, E.M. and R.C. Reuter, Jr. 1965. "Crack Extension in Fiberglass Reinforced Plastics." T/AM 275. Dept of Theor & Appl Mech, University of Illinois.
25. Yan, X.Q., S.Y. Du, and D.U.O. Wang. 1991. "An Engineering Method of Determining the Delamination Fracture Toughness of Composite Laminates." *Eng Frac Mech*, 39(4):623-627.
26. Hahn, H.T. 1983. "A Mixed-Mode Fracture Criterion for Composite Materials." *Comp Tech Rev*, 5:26-29.
27. Hahn, H.T. and T. Johnnesson. 1983. "A Correlation between Fracture Energy and Fracture Morphology in Mixed-Mode Fracture of Composites," in *Mechanical Behaviour of Materials - IV* Stockholm. pp. 431-438.
28. Donaldson, S.L. 1985. "Fracture Toughness Testing of Graphite/Epoxy and Graphite/Peek Composites." *Composites*, 16(2):103-112.
29. White, S.R. 1987. "Mixed-Mode Interlaminar Fracture of Graphite/Epoxy," Washington University.
30. Hashemi, S. and A.J. Kinloch. 1987. "Interlaminar Fracture of Composite Materials," in *6th ICCM & 2nd ECCM*, F.L. Matthews, et al., Eds. Elsevier Applied Science, New York. pp. 254-264.
31. Hashemi, S. and A.J. Kinloch. 1990. "The Effects of Geometry, Rate and Temperature on the Mode I, Mode II and Mixed-Mode I/II Interlaminar Fracture of Carbon-Fibre/Poly(Ether-Ether Ketone) Composites." *J Comp Mat*, 24:918-956.
32. Hashemi, S. and J.G. Williams. 1991. "Mixed-Mode Fracture in Fiber-Polymer Composite Laminates," in *Composite Materials: Fatigue and Fracture, Vol. 3, ASTM STP 1110*, T.K. O'Brien, Ed. ASTM Int., W. Conshohocken, PA.
33. Gong, X.-J. and M. Benszeggagh. 1995. "Mixed Mode Interlaminar Fracture Toughness of Unidirectional Glass/Epoxy Composite," in *Composite Materials: Fatigue and Fracture, Vol. 3, ASTM STP 1230*, R.H. Martin, Ed. ASTM Int., W. Conshohocken, PA. pp. 100-123.
34. Reeder, J.R., et al. 2002. "Postbuckling and Growth of Delaminations in Composite Plates Subjected to Axial Compression," in proceeding of the *43rd AIAA/ASME/ASCE/AHS/ASC Structures, Structural Dynamics, and Materials Conference*. Denver, AIAA-2002-1746.
35. Shindo, Y., et al. 2005. "Analysis and Testing of Mixed-Mode Interlaminar Fracture Behavior of Glass-Cloth/Epoxy Laminates at Cryogenic Temperatures." *J Eng Mat Tech*, 127(4):468-475.
36. Ducept, F., P. Davies, and D. Gamby. 1997. "An Experimental Study to Validate Tests Used to Determine Mixed Mode Failure Criteria of Glass/Epoxy Composites." *Comp Pt A–Appl Sci & Man*, 28(8):719-729.
37. Goyal, V.K., E.R. Johnson, and C.G. Davila. 2004. "Irreversible Constitutive Law for Modeling the Delamination Process Using Interfacial Surface Discontinuities." *Comp Struct*, 65(3-4):289-305.
38. "VCCT for ABAQUS User's Manual, Version 1.1." 2005. ABAQUS, Inc.
39. Engelstad, S.P., et al. 2005. "A High Fidelity Composite Bonded Joint Analsys Validation Study–Part I: Analysis," in proceeding of the *46th AIAA/ASME/ASCE/AHS/ASC Structures, Structural Dynamics, and Materials Conference*. Austin, TX, AIAA 2005-2166.

Equation labeled as footnotes

1

2

3

4

5

6

7